Reaction of $LiAr^{Me6}$ (Ar^{Me6} = C_6H_3-2,6-(C_6H_2-2,4,6-Me_3)$_2$) with Indium(I)chloride Yields Three *m*-Terphenyl Stabilized Mixed-Valent Organoindium Subhalides

Petra Vasko,[a] Akseli Mansikkamäki,[a] James C. Fettinger,[b] Heikki M. Tuononen,[a,*] and Philip P. Power[b,*]

[a]*Department of Chemistry, NanoScience Center, University of Jyväskylä, P.O. Box 35. FI-40014, University of Jyväskylä, Finland.*

[b]*Department of Chemistry, University of California, One Shields Avenue, Davis, CA 95616, United States.*

ABSTRACT

Indium(I)chloride reacts with $LiAr^{Me6}$ (Ar^{Me6} = C_6H_3-2,6-(C_6H_2-2,4,6-Me_3)$_2$) in THF to give three new mixed-valent organoindium subhalides. While the 1:1 reaction of InCl with $LiAr^{Me6}$ yields the known metal-rich cluster $In_8(Ar^{Me6})_4$ (**1**), the use of freshly prepared $LiAr^{Me6}$ led to incorporation of iodide, derived from the synthesis of $LiAr^{Me6}$, into the structures, to afford $In_4(Ar^{Me6})_4I_2$ (**2**) along with minor amounts of $In_3(Ar^{Me6})_3I_2$ (**3**). When the same reaction was performed in 4:3 stoichiometry, the mixed-halide compound $In_3(Ar^{Me6})_3ClI$ (**4**) was obtained. Further increasing the chloride:aryl ligand ratio resulted in the formation of the known mixed-halide species $In_4(Ar^{Me6})_4Cl_2I_2$ that can also be obtained from the reaction of InCl with *in situ* prepared $LiAr^{Me6}$ in toluene. The new compounds **2** and **4** were characterized in the solid state by X-ray crystallography and IR spectroscopy, and in solution by UV/Vis and $^1H/^{13}C\{^1H\}$ NMR spectroscopies. The structural characterization of **2** and **4** was supported by electronic structure calculations at the density functional level of theory which were also performed to rationalize the cluster-type bonding in **1**.

KEYWORDS

organoindium subhalides, mixed-valent compounds, molecular clusters, X-ray crystallography, DFT calculations

INTRODUCTION

Isolable organo main group clusters have attracted much attention in the past decades and the number of heavier group 13 element clusters in particular has increased rapidly [1−7]. However, the mechanisms of their formation are neither straightforward nor easy to explain [5,6], and both the reaction yield and the number of side products show significant variation in response to small changes in reaction conditions [3]. Nevertheless, the study of clusters of the heavier main group elements is of importance because of their interesting structures, solid state properties, and potentially unique reactivity. For example, we demonstrated recently that the tin species $Sn_8(Ar^{Me6})_4$ (Ar^{Me6} = C_6H_3-2,6-(C_6H_2-2,4,6-Me_3)$_2$) is the first organo main group cluster known to perform small molecule activation under ambient conditions[8], thereby mimicking the reactivity typical for transition metals [9]. Another valuable attribute of organo main group clusters is that they feature the elements in low oxidation states and incorporate unsaturated metals whose coordination environments resemble those of the respective atoms at elemental surfaces[10].

For the group 13 elements, indium is distinguished from its lighter congeners aluminum and gallium by the fact that the low oxidation state halides InX (X = Cl, Br, or I) are all commercially available. Despite such easy access to useful starting materials, less than 100 compounds containing one or more In−In bonds have been structurally characterized [11]. Structural data are even sparser for indium clusters with only a handful of reported examples whose composition has been verified by X-ray crystallography [2,12–20]. It should be noted that none of these compounds bears resemblance to the large anionic aluminum or gallium clusters of Schnöckel [21,22], and only a number of them incorporate indium atoms at different oxidation states. Mixed-valent metal clusters are interesting species as they may undergo subsequent substitution reactions or other postsynthetic modifications to their structure.

In 2000, we reported the isolation and structural characterization of $In_8(Ar^{Me6})_4$ (**1**) [2], a metal-rich indium cluster with a slightly distorted cubane structure. It was synthesized by the reaction of $LiAr^{Me6}$ with InCl in an approximately 1:1 ratio. This result is in contrast to the corresponding reaction of InCl with the bulkier terphenyl lithium reagents $LiAr^{Pri4}$ or $LiAr^{Pri6}$ (Ar^{Pri4} = C_6H_3-2,6(C_6H_3-2,6-Pr^i_2)$_2$; Ar^{Pri6} = C_6H_3-2,6-(C_6H_2-2,4,6-Pr^i_3)$_2$), which afforded monomeric $InAr^{Pri6}$ [23] or dimeric $Ar^{Pri4}InInAr^{Pri4}$ [19]. The structural relationship of **1** to the tin cluster $Sn_8(Ar^{Me6})_4$ makes it a very interesting target for further reactivity studies. While exploring this possibility in detail, we noticed that the preparation of **1** is very sensitive to the reaction conditions employed and can easily afford other products. Herein we describe the results of our investigations detailing the synthesis and characterization of two new mixed-valent organoindium subhalides $In_4(Ar^{Me6})_4I_2$ (**2**) and $In_3(Ar^{Me6})_3ClI_2$ (**4**) (see Scheme 1) along with the crystallographic structure determination of $In_3(Ar^{Me6})_3I_2$·THF (**3**), a minor byproduct in the synthesis of **2**. Compound **2** has a unique tetrametallic molecular structure with two bridging iodides, while **4** contains a planar In_3Cl core with a terminal In−I bond that is essentially perpendicular to the four-membered ring. The reported experimental data are augmented with computational results at the density functional level of theory, including the description of bonding in cluster **1**.

Scheme 1. Reactions of $LiAr^{Me6}$ with InCl under different reaction conditions.

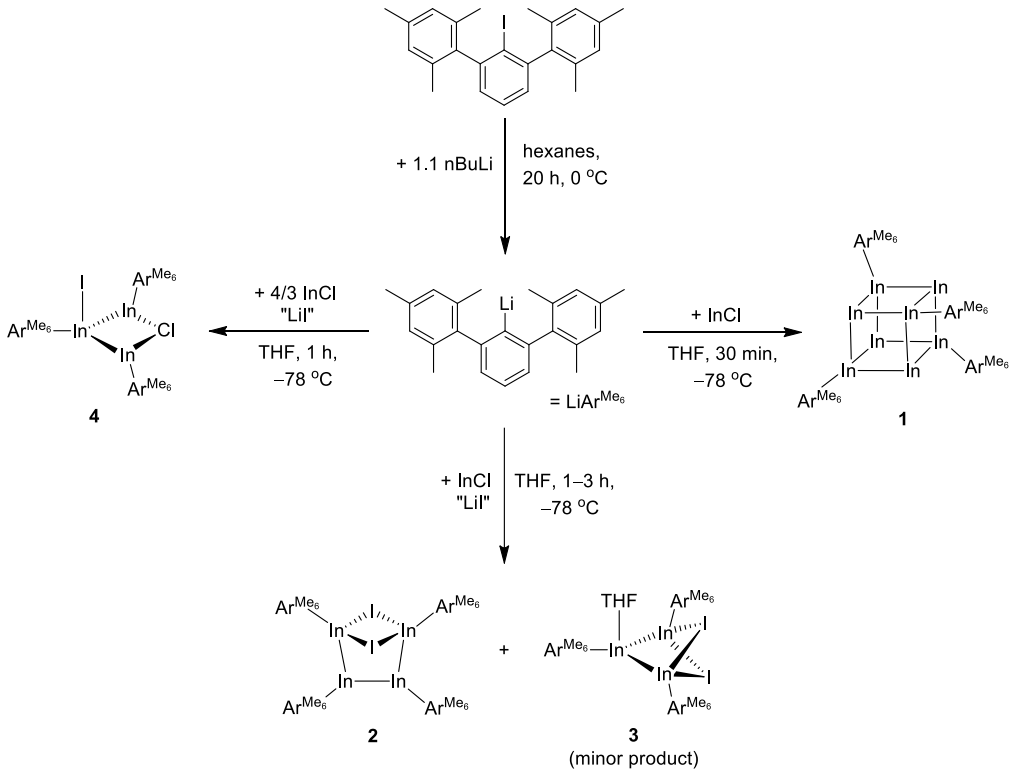

EXPERIMENTAL SECTION

General Procedures. All manipulations were carried out under anaerobic and anhydrous conditions by using modified Schlenk line techniques under a dinitrogen/argon atmosphere or in a drybox. Solvents were first dried and then stored over sodium. Unless otherwise stated, all materials were obtained from commercial sources and used as received. $Ar^{Me6}I$ was prepared according to a literature procedure[24]. $LiAr^{Me6}$ was prepared from $Ar^{Me6}I$ by lithiation with 1.1 eq. of Li^nBu in hexanes at 0 °C. The reaction mixture was stirred overnight at room temperature after which the solution was decanted. The off-white precipitate was washed twice with hexanes and dried under vacuum at room temperature for 2 h.

All physical measurements were carried out under strictly anaerobic and anhydrous conditions. ^1H and $^{13}C\{^1H\}$ NMR spectra were collected on Varian 400 or 600 MHz spectrometers and referenced to known standards. IR spectra were recorded as Nujol mulls between CsI plates on a Perkin-Elmer 1430 radio recording infrared spectrometer. UV-Visible spectra were recorded from dilute solutions in hexanes using a 3.5 mL quartz cuvette and an Olis 17 modernized Cary 14 UV/Vis/NIR spectrophotometer. Melting points were determined on a Meltemp II apparatus using glass capillaries sealed with vacuum grease, and are uncorrected. Elemental analyses were performed by using an Elementar Analysensysteme GmbH Vario EL *III* element analyzer.

Synthesis of $In_4(Ar^{Me6})_4I_2$ (2). 0.82 g (5.5 mmol) of InCl was dissolved in 10 mL of THF at *ca.* −78 °C. 1.60 g (5 mmol) of freshly prepared $LiAr^{Me6}$ was dissolved in 30 mL of THF, cooled to *ca.* 0 °C and added dropwise to the InCl solution. The dark orange mixture was stirred for 1.5 h at *ca.* −78 °C and warmed to *ca.* 0 °C. After evaporation of the solvent, the residue was extracted to *ca.* 50 mL of hexanes and filtered. Approximately 20 mL of hexanes was evaporated to incipient crystallization. Storage at *ca.* 6 °C overnight produced **2** as brown crystals of sufficient quality for X-ray diffraction studies. Yield 1.25 g (46 % with respect to In). Mp: 75–76 °C (dec). ^1H NMR (C_6D_6, 600 MHz): δ = 1.78 (br s, 24H,

Mes-CH_3), 2.18 (s, 24H, Mes-CH_3), 2.36(s, 24H, Mes-CH_3), 6.89 (s, 16H, *m*-Mes), 6.96 (d, $^3J_{HH}$ = 12 Hz, 8H, *m*-C$_6H_3$), 7.19 (t, $^3J_{HH}$ = 12 Hz, 4H, *p*-C$_6H_3$). $^{13}C\{^1H\}$ NMR (C_6D_6, 151 MHz): δ = 21.84, 22.17 (Mes-*C*H$_3$), 128.35 (*m*-Mes), 129.64 (*m*-C$_6$H$_3$), 135.79 (*o*-Mes), 136.65 (*p*-C$_6$H$_3$), 137.20 (*p*-Mes), 137.35 (*ipso*-Mes), 141.54 (*o*-C$_6$H$_3$), 148.20 (*ipso*-C$_6$H$_3$). IR in Nujol mull (cm^{-1}) with CsI plates: 240, 270, 320. UV-Vis (hexanes, nm, ε): 496 (2200). Elemental analysis for $C_{96}H_{100}In_4I_2$: Calculated: C: 58.62 and H: 5.12; Found: C: 58.39 and H: 5.16.

Synthesis of In$_3$(Ar^{Me6})$_3$ClI (4). 1.00 g (6.7 mmol) of InCl was dissolved in 10 mL of THF at *ca.* −78 °C. 1.60 g (5 mmol) of freshly prepared LiAr^{Me6} was dissolved in 30 mL of THF, cooled to *ca.* 0 °C with an ice bath and added dropwise to the InCl solution. The dark orange mixture was stirred for 1 h at *ca.* −78 °C and warmed up to *ca.* 0 °C. After evaporation of the solvent, the residue was extracted to 50 mL of hexanes and filtered. Approximately 20 mL of hexanes was evaporated to incipient crystallization. Storage at *ca.* 6 °C overnight produced **4** as yellow crystals of sufficient quality for X-ray diffraction studies. Yield 0.66 g (28 % with respect to In). Mp: 100−102 °C (dec). ^{1}H NMR (C_6D_6, 600 MHz): δ = 2.01 (s, 6H, Mes-CH_3), 2.04 (s, 6H, Mes-CH_3), 2.16 (s, 18H, Mes-CH_3), 2.18 (s, 6H, Mes-CH_3), 2.24 (s, 6H, Mes-CH_3), 2.29 (s, 12H, Mes-CH_3), 6.74 (s, 4H, *m*-Mes), 6.86 (d, under the singlet at 6.88 ppm, 2H, *m*-C$_6H_3$), 6.88 (s, 8H, *m*-Mes), 6.97 (d, $^3J_{HH}$ = 6 Hz, 4H, *m*-C$_6H_3$), 7.20 (t, $^3J_{HH}$ = 6 Hz, 2H, *p*-C$_6H_3$). $^{13}C\{^1H\}$ NMR (C_6D_6, 151 MHz): δ = 21.42, 21.53, 21.64, 21.67, 21.91, 22.01 (Mes-*C*H$_3$), 127.29, 127.98, 128.14 (*m*-Mes), 128.35, 129.00, 129.32 (*m*-C$_6$H$_3$), 129.43, 129.64, 129.79 (*o*-Mes), 135.79, 136.12, 136.18 (*p*-C$_6$H$_3$), 136.30, 137.02, 137.38 (*p*-Mes), 141.10, 141.63, 142.11 (*ipso*-Mes), 148.27, 148.74, 149.23 (*o*-C$_6$H$_3$), 156.63, 163.20, 165.89 (*ipso*-C$_6$H$_3$). IR in Nujol mull (cm^{-1}) with CsI plates: 240, 250, 315, 490, 530, 560. UV-Vis (hexanes, nm, ε): 342 (3500). The extreme sensitivity of crystalline **4** prevented an accurate elemental analysis of the sample.

X-Ray Structure Determination. Crystal data and structure refinement parameters are shown in Table 1. Suitable crystals were selected and covered with a layer of hydrocarbon oil under a rapid flow of dinitrogen. They were mounted on a synthetic micro loop attached to a goniometer base and placed on the goniometer head in a cold N_2 stream on the diffractometer. X-ray data for **2**–**4** were collected at 90(2) K with (λ= 0.71073 Å) Mo $K_{\alpha1}$ radiation using a Bruker APEX II diffractometer in conjunction with a CCD detector. The collected reflections were corrected for Lorentz and polarization effects and for absorption by use of Blessing's method as incorporated into the program SADABS [25]. The structures were solved by direct methods and refined with the SHELXL software package [26]. Refinement was by full-matrix least-squares procedures with all carbon-bound hydrogen atoms included in calculated positions and treated as riding atoms.

Computational Details. All calculations were performed with Turbomole [27] and ADF program packages [28] using density functional theory. Geometries of compounds **2**, **4,** and **1′** were optimized with the hybrid PBE0 exchange correlation functional [29−32] in combination with def2-TZVP basis sets[33] and empirical DFT-D3 dispersion correction [34] with Becke-Johnson damping [35]. Orbital analysis was performed for the optimized geometry of **1'** with the ADF program suite using the PBE0 functional and all-electron TZ2P basis sets [36]. Scalar relativistic effects were taken into account through the zeroth-order regular approximation (ZORA)[37−39] as implemented in ADF. Localized Kohn-Sham orbitals of **1′** were generated from the PBE0/def2-TZVP determinant using Boys' localization criteria [40].

Table 1. Crystal Data and Refinement Summary for **2**·C_6H_{14}, **3**, and **4**.

	2·C_6H_{14}	**3**	**4**
formula	$C_{99}H_{107}I_2In_4$	$C_{84}H_{99}I_2In_3O_3$	$C_{72}H_{75}ClIIn_3$
fw (g mol^{-1})	2009.92	1754.89	1447.13
crystal system	monoclinic	orthorhombic	monoclinic
space group	$P2_1/n$	$Pca21$	$C2/c$
a (Å)	13.2709(14)	23.737(3)	15.748(5)
b (Å)	26.271(3)	13.9250(15)	18.215(6)
c (Å)	24.583(3)	22.458(2)	22.542(8)
α (°)	90	90	90
β (°)	99.7294(18)	90	99.457(5)
γ (°)	90	90	90
V (Å^3)	8447.1(16)	7422.9(14)	6378(4)
Z	4	4	4
T (K)	90(2)	90(2)	90(2)
cryst. size (mm)	0.139×0.080 ×0.037	0.238×0.148 ×0.074	0.203×0.108 ×0.097
F(000)	4012	3520.0	2896
ρ_{calc} (g cm^{-3})	1.580	1.570	1.507
μ (mm^{-1})	1.856	1.804	1.641
$2\theta_{max}$ (°)	25.461	25.995	27.511
reflns. collected	60567	80350	28306
unique reflns.	15591	14530	7338
R_{int}	0.1143	0.0630	0.0501
reflns. [$I>2\sigma(I)$]	9877	12822	6094
R_1 [$I>2\sigma(I)$]	0.0519	0.0328	0.0459
wR_2 (all data)	0.1370	0.0675	0.1040
GoF (F^2)	1.014	1.040	1.160

RESULTS AND DISCUSSION

Cluster **1** was synthesized by treating a suspension of InCl in THF with one equivalent of the lithium aryl, $LiAr^{Me6}$ [42], at −78 °C, giving a dark orange brown solution. After stirring for 30 min and subsequent workup, red crystals of **1** were isolated [2]. However, if the $LiAr^{Me6}$ reagent is freshly prepared and kept at 0 °C, and its reaction time with InCl exceeds 30 min at −78 °C, a dark orange-brown solution with an almost black precipitate, presumably indium metal, formed. After workup and crystallization, compound **2** could be obtained as dark brown crystals. Crystals of **2** are stable in the solid state but decompose to indium metal and other products of undetermined composition upon prolonged standing in solution at room temperature.

The Structure of 2. Compound **2** crystallizes in a monoclinic $P2_1/n$ space group with a half of a crystallization solvent (hexane) in the asymmetric unit. The solid state structure of **2** turned out to be quite interesting and was initially assumed to contain a bicyclo[2.1.1]hexane-type core of six indium atoms. Even though this structural model gave an excellent fit to the experimental X-ray diffraction data (see Supplementary data), bridging indium atoms are unprecedented in the literature. For this reason, the possibility that the bicyclic core in **2** is formed by four indium and two iodine atoms was also considered (Figure 1). The incorporation of iodide in Ar ligand systems has been observed before for *in situ* prepared $LiAr^{Me6}$ (from ^{n}BuLi and $Ar^{Me6}I$) which afforded the mixed halide product $In_4(Ar^{Me6})_4Cl_2I_2$ (**5a**) upon reaction with InCl in toluene [20].

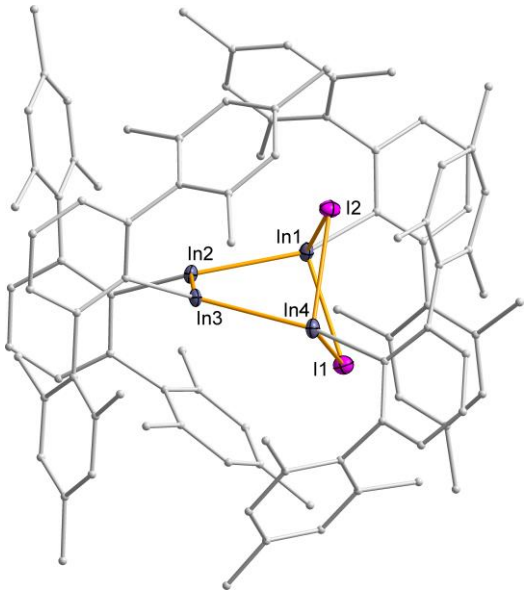

Figure 1. X-ray crystal structure of **2**. Crystallization solvent, hydrogen atoms, and disorder related to indium and iodine positions are not shown for clarity. Thermal ellipsoids are drawn at 30% probability level. Selected bond lengths (Å) and angles (°): In(1)-In(2): 2.7806(13), In(1)-I(1): 2.9212(14), In(1)-I(2): 2.9214(12), In(2)-In(3): 2.8565(16), In(3)-In(4): 2.8165(14), In(4)-I(1): 2.9296(14), In(4)-I(2): 2.9635(12), In(1)-In(2)-In(3): 102.26(5), In(2)-In(3)-In(4): 101.10(5), In(1)-I(1)-In(4): 89.48(3), In(1)-I(2)-In(4): 88.82(4), In(2)-In(1)-I(1): 92.36(4), In(2)-In(1)-I(2): 92.30(4), In(3)-In(4)-I(1): 101.58(7), In(3)-In(4)-I(2): 81.72(6), I(1)-In(1)-I(2): 86.05(4), I(1)-In(4)-I(2): 85.14(4), In(1)-In(2)-In(3)-In(4): −21.49(9).

A reinterpretation of the experimental diffraction data for **2** using a bicyclic In_4I_2 core resulted in a very good fit though the important statistical parameters are poorer than what was found for the all-indium model (see Supplementary data). Thus, the X-ray data alone does not allow a distinction between the two possibilities. The extant spectroscopic data for **2** (NMR, IR, and UV/Vis) provides no further structural information, for which reason a computational analysis was performed. Full geometry optimizations using dispersion corrected DFT functional (PBE0-D3/def2-TZVP)[29−35] showed the calculated structure of $In_4(Ar^{Me6})_4I_2$ to be in very good agreement with the X-ray data (see Supplementary data), while optimization for $In_6(Ar^{Me6})_4$ led to collapse of the bicyclo[2.1.1]hexane-type core and reorganization of the metal−metal interactions. This strongly suggests that the two bridging nuclei in the structure of **2** are halides that originated from "LiI" derived from the synthesis of the lithium aryl reagent $LiAr^{Me6}$. The computational results are further supported by elemental analysis data for **2** that perfectly match the formula $In_4(Ar^{Me6})_4I_2$. If $LiAr^{Me6}$ was used *in situ* for the synthesis of **2**, a colorless solution and a maroon insoluble and intractable precipitate was obtained after workup.

The structure of **2** has four indium atoms of which two have trigonal planar (In(2) and In(3)) and two have distorted tetrahedral (In(1) and In(4)) coordination (Figure 1). The In−In distances in **2** lie between 2.7806(13) and 2.8565(16) Å, whereas the In−I bond lengths are slightly longer and span a smaller range of distances from 2.9212(14) to 2.9635(12) Å. It is evident that two of the indium atoms (In(1) and In(4)) have oxidation state +2 and the remaining two (In(2) and In(3)) +1. Hence, some disproportionation of In^I has taken place, which is supported by the formation of a dark precipitate during the reaction. The structure of **2** is unique but it is related to the mixed-valent compound $In_4(C(SiMe_3)_3)_4Br_2$ (**6**) reported by Uhl and coworkers [42]. The average indium oxidation state in **6** is the same as that in **2**,

but one of the two bromides is triply bridging for which reason the indium atoms do not adopt a planar geometry but form a tetrahedron. The differences in the structures of compounds **2** and **6** may simply be due to the different steric bulk of the Ar^{Me6} ligand in **2** in comparison to that of the tris(trimethylsilyl)methyl group in **6**.

Chart 1. Structures of compounds **5**–**9**.

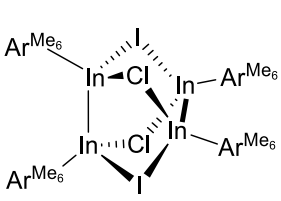

5a

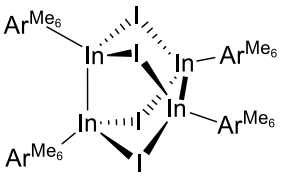

5b

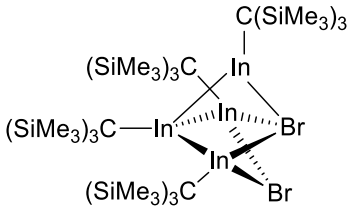

6

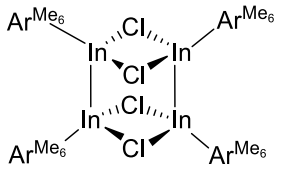

7

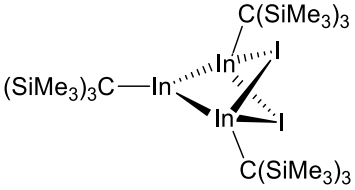

8

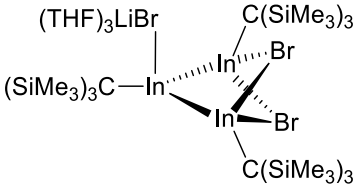

9

The structure of **2** can also be compared to that of $In_4(Ar^{Me6})Cl_4$ (**7**) which is formed by reacting $LiAr^{Me6}$ with InCl in toluene.[20] The similarities in the structures of **2** and **7** suggest that the remaining In^I centers in **2** (In(2) and In(3)) could be oxidized to form the tetraiodo compound $In_4(Ar^{Me6})I_4$ with a structure similar to that known for **7**; a structural isomer of $In_4(Ar^{Me6})_4I_4$ in which the two In−In bonds are oriented perpendicularly to each other (**5b**) has been reported [20]. However, no indication of the formation of $In_4(Ar^{Me6})I_4$ was seen under the employed reaction conditions even when the reaction time was extended to 3 hours. Furthermore, attempts to oxidize **2** with a stoichiometric amount of I_2 gave a mixture of unknown products and indium metal. It is likely that iodine not only oxidizes the In^I centers in **2** but also cleaves the In−C bonds, thereby leading to decomposition [17].

Interestingly, the synthesis of **2** also yielded a few pale yellow needle-like crystals that could be separated from **2** under a microscope. The crystals were of X-ray quality and a subsequent structure determination showed them to be that of $In_3(Ar^{Me6})_3I_2$·THF (**3**). The structure of **3** contains a chain of the indium atoms in which a molecule of the reaction solvent (THF) is coordinated to the central indium atom and two iodide bridges link the terminal indium nuclei (Figure 2). Thus, all indium atoms in **3** are coordinatively saturated. The In−In distances in **3** are in the normal range of In−In single bonds and fully comparable to those in a related compound $In_3(C(SiMe_3)_3)_3I_2$ (**8**) described by Uhl [17]. The key structural difference between **3** and **8** is the coordinatively unsaturated indium atom in the latter species. The structure of **3** can also be compared with the anion in the salt $[Li(THF)_3][In_3(C(SiMe_3)_3)_3Br_3]$ (**9**) that is formed as a byproduct in the synthesis of the tetrahedral tetraindium cluster $In_4(C(SiMe_3)_3)_4$ from stoichiometric amount of InBr and $LiC(SiMe_3)_3$ [18]. The structural similarity of byproducts **3** and **9** suggests a common mechanism for their formation from two closely related reactions.

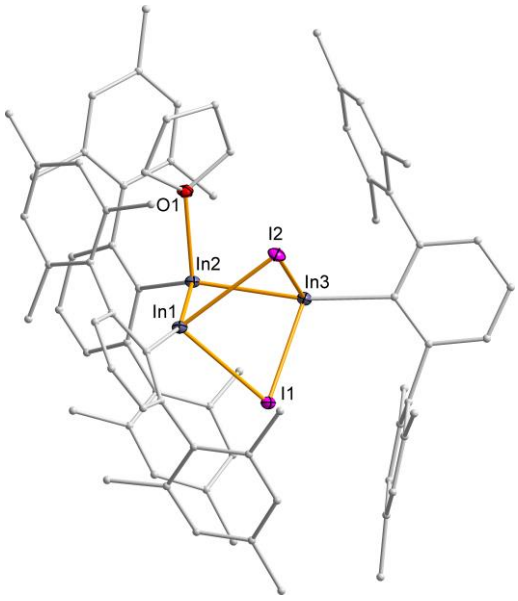

Figure 2. X-ray crystal structure of **3**. Uncoordinated solvent molecules and hydrogen atoms are not shown for clarity. Thermal ellipsoids are drawn at 30% probability level. Selected bond lengths (Å) and angles (°): In(1)-In(2): 2.8148(7), In(2)-In(3): 2.7992(8), In(1)-I(1): 2.9393(8), In(1)-I(2): 3.0451(8), In(3)-I(1): 2.9271(7), In(3)-I(2): 3.0741(7), In(1)-In(2)-In(3): 82.24(2), In(1)-I(1)-In(3): 77.999(19), In(1)-I(2)-In(3): 74.214(18), I(1)-In(1)-I(2): 82.62(2), I(1)-In(3)-I(2): 82.316(19).

The mechanism for the formation of **2** is currently unknown. It is plausible that the cubane cluster **1** is initially formed but then decomposes because of the longer reaction time used. The formation of **2** over $In_4(Ar^{Me6})_4$ can be rationalized by the presence of "LiI" in the reaction mixture along with the steric requirements of the Ar^{Me6} ligand that are likely to make the tetrahedral core in $In_4(Ar^{Me6})_4$ energetically unfavorable. However, it is less obvious why **2** (or **3**) contains only iodine, while the reaction of InCl with $LiAr^{Me6}$ in toluene yields the chloride compound **7**, the mixed halide species **5a** and its all-iodine analogue **5b**, as well as the cubane cluster **1** [20]. For this reason, the effect of stoichiometry to the incorporation of chlorine into the reaction products was evaluated in detail.

The aryl reagent $Li(Ar^{Me6})$ was prepared similarly as in the synthesis of **2** and added to a solution of InCl in varying amounts. When an excess of InCl was used, the reaction mixture became dark orange after stirring for 1 h. Subsequent workup gave an intense dark yellow solution in hexanes which was reduced in volume and placed in a *ca.* 6 °C refrigerator to incipient crystallization. Compound **4** was harvested as intensely colored yellow crystals that are unstable and soon become coated with a grey insoluble powder. In polar solvents and at room temperature, **4** forms a grey powdery precipitate within a matter of minutes.

The Structure of 4. Compound **4** crystallizes in a monoclinic *C*2/*c* space group with half a molecule in the asymmetric unit (Figure 3). Three indium atoms and a chloride form a planar four-membered ring in which each indium is also bound to an Ar^{Me6} ligand. In addition, In(2) is bound to a terminal iodine atom that is disordered over two equivalent positions, one above and one below the In_3Cl plane. The structure of **4** formally contains the dicationic $[In_3(Ar^{Me6})_3]^{2+}$ core in which the oxidation state of In(1)/In(1′) is +2 and that of In(2) is +1, indicating disproportionation as in compound **2**. The incorporation of both chloride and iodide in the structure of **4** is consistent with the increase in the chloride:aryl ligand ratio in the synthesis.

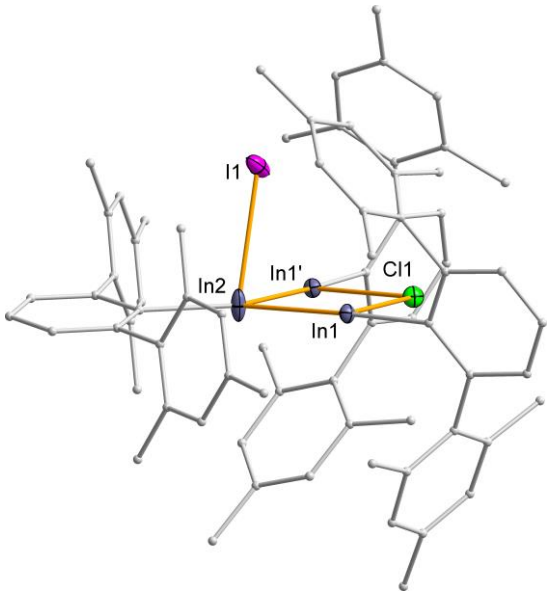

Figure 3. X-ray crystal structure of **4**. Hydrogen atoms are not shown for clarity. I(1) is disordered with 50 % occupancy; the I(1') position below the In(1')-In(2)-In(1) plane is not shown. Thermal ellipsoids are drawn at 30% probability level. Selected bond lengths (Å) and angles (°): In(1)-In(2): 2.7777(7), In(1)-Cl(1): 2.6574(13), In(2)-I(1): 2.9947(10), Cl(1)-In(1)-In(2): 88.49(4), In(1)-In(2)-In(1′): 88.91(3), In(1)-In(2)-I(1): 88.15(3), In(1′)-In(2)-I(1): 76.24(3).

The structure of **4** can be compared to that of the minor byproduct **3**. It is evident that the two compounds are closely related to one another and also to **8** and **9** [17]. The In–In bond lengths in **4** are slightly shorter than those in **3**, **8**, or **9**, in agreement with the change in the coordination number of the metal atoms. While both **3**, **8**, and **9** all have a doubly halide bridged structure, only the chloride anion is bridging in **4** and the iodide is terminally bound to In(2) as exemplified by the I(1)–In distances 2.9947(10), 3.568(1), and 4.019(1) Å to In(2), In(1′), and In(1), respectively. The difference in the binding mode of the heavier halide can simply be due to the significant size disparity between I^- and Cl^- which makes a doubly bridged energetically unfavorable for **4**. In line with this assumption, there are only six structurally characterized examples of M(μ_2-Cl)(μ_2-I)M bonding in the Cambridge Structural Database (M = any metal) [11]. In **4**, crystallographic symmetry enforces the *ipso* carbon of Ar^{Me6} ligand at In(2) to be on the same plane with the In_3Cl ring. However, optimizations conducted at the PBE0-D3/def2-TZVP level of theory[29–35] showed that the geometry of **4** is only slightly puckered even when not in a crystalline environment (see Supplementary data): the calculated dihedral angles Cl(1)-In(1)-In(2)-In(1′) and In(1)-C(*ipso*)-In(1′)-In(2) are 8.6 and −18.1°, respectively. As a whole, the optimized metrical parameters of **4** are in very good agreement with the X-ray data.

The formation of **4** required only a minor excess of InCl. If the amount of InCl was increased further, a different product was again obtained. Using a 5:3 stoichiometry of the reactants InCl and $LiAr^{Me6}$ gave a golden yellow solution and a black precipitate. The solution afforded significant amounts of light yellow X-ray quality crystals after extraction in hexanes, filtration, and standing for overnight at *ca*. 6 °C. A subsequent structure determination revealed the product as the known mixed-halide species **5a**. No other characterizable products could be obtained from the reaction even when using greater amounts of InCl.

In addition to the synthesis and characterization of organoindium subhalides **2** and **4**, we also investigated the electronic structure of cluster **1** to rationalize its bonding. The approximately snub disphenoid geometry of **1** is well in line with Wade-Mingos rules for 4*n*-like species with 8 vertices. The local symmetry of the metallic In_8 core in **1** is close to D_{2d} point group with minor distortions attributable to

the steric bulk of the Ar^{Me6} ligands. This is supported by geometry optimization (PBE0-D3/def2-TZVP)[29–35] of the parent species In_8H_4 (**1′**) that yields a perfectly D_{2d} symmetric structure. Thus, the Ar^{Me6} ligands stabilize **1** by almost completely obscuring the surface of the metallic core from attack, but the steric bulk of the ligands has virtually no influence on the overall geometry of the cluster. For this reason, we performed detailed bonding analyses only for the parent species In_8H_4.

The point group of a perfectly cubical In_8H_4 cluster would be T_d with eight symmetry-equivalent indium atoms. Since the snub disphenoid structure of **1′** has D_{2d} point group, not all indium atoms in it are related by symmetry. Consequently, there are two types of In–In bonds in **1′** and its electronic structure can be conveniently described by considering interactions both within and between four equivalent In–In–H fragments. The occupied valence Kohn-Sham orbitals of a single In–In–H fragment (Figure 4) consist of three σ-type orbitals housing three electron pairs and one half occupied π-type orbital that is bonding within the fragment plane (π_{IP}). The lowest virtual orbitals of the fragment are all of π-type either within the fragment plane (π^*_{IP}) or perpendicular to it (π_{OP} and π^*_{OP}). It is evident that In–In bonding in the fragment is relatively weak as one of the σ-type orbitals is antibonding and the bonding π_{IP} orbital is only half occupied.

Figure 4 shows a qualitative orbital correlation diagram connecting the orbitals of four equivalent In–In–H fragments to those of **1′**. Orbitals $34a_1$ and $34b_2$ as well as those in the degenerate set $48e$ are mostly non-bonding or In–H bonding, while the remaining ten occupied orbitals describe different In–In interactions. For example, orbital $15b_1$ shows a cluster-type bonding interaction between fragment π_{OP} orbitals, whereas orbital $33a_1$ is the symmetric combination of fragment σ-orbitals and displays both intra- as well as interfragment, cluster-type, In–In bonding. A cluster-type bonding interaction is also shown by orbital $36a_1$ which displays some non-bonding character as well. Orbitals $47e$ and $35b_2$ are combinations of σ-type fragment orbitals describing intrafragment In–In (and In–H) bonding, while orbitals $33b_2$, $49e$, and $35a_1$ are combinations of both σ- and π-type fragment orbitals with interfragment In–In bonding character.

Taken together, out of the 14 occupied orbitals in cluster **1′**, only six describe In–In bonding between the four equivalent In–In–H fragments. This result is corroborated by the analysis of localized orbitals for **1′** (see Supplementary data). The localization procedure yields six orbitals with multicenter bonding character as well as eight 2c–2e orbitals that correspond to the H–In and In–In bonds in four In–In–H fragments. The multicenter bonding orbitals are of two types: four orbitals describe 3c–2e In–In interactions between the In–In–H fragments, while the remaining two are more delocalized and depict cluster-type bonding similar to that in Kohn-Sham orbitals $35a_1$, $15b_1$, and $36a_1$. Furthermore, the orbitals describing the 3c–2e In–In interactions are most localized at the terminal In centers of each In–In–H fragment, suggestive of lone pair character in addition to their bonding nature.

The orbital diagram in Figure 4 shows that the frontier orbitals of **1′** have appropriate morphologies to react with both Lewis acids and bases. For example, the HOMO (orbital $36a_1$) has some lone pair character at each In^0 center which are also the sites that contribute the most to the shapes of the degenerate LUMOs (orbitals $50e$). Consequently, **1′** and, by implication, cluster $In_8(Ar^{Me6})_4$ may well react with small molecules similarly to $Sn_8(Ar^{Me6})_4$. More detailed studies of the reactivity of $In_8(Ar^{Me6})_4$ are currently underway.

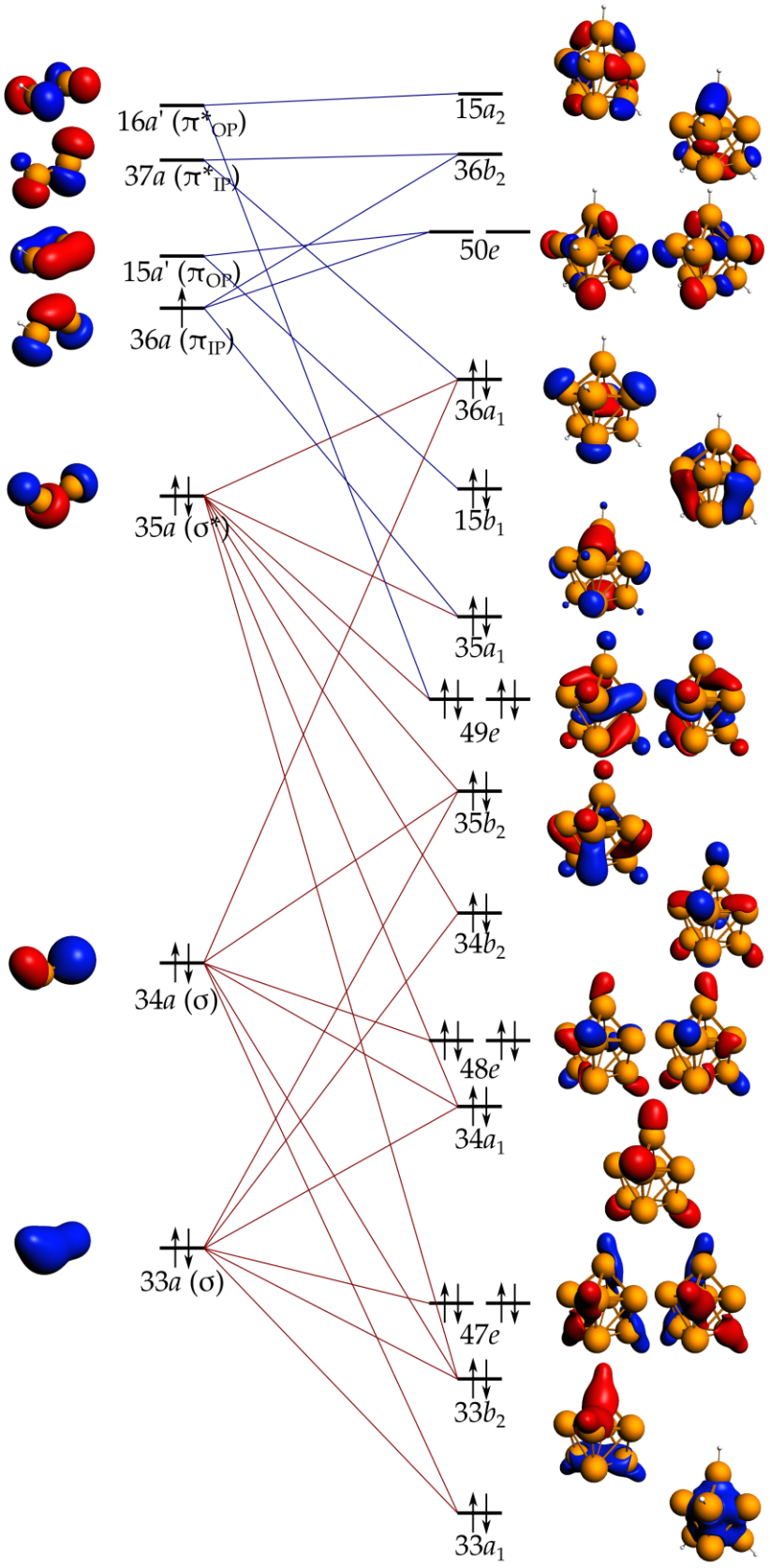

Figure 4. Qualitative orbital correlation diagram connecting the valence orbitals of In_2H fragment (left) to those of In_8H_4 (right).

CONCLUSIONS

In this work, we have examined the reaction between InCl and $LiAr^{Me6}$ under different reaction conditions. The results describe the synthesis and complete characterization of two new *m*-terphenyl stabilized organoindium subhalides $In_4(Ar^{Me6})_4I_2$ (**2**) and $In_3(Ar^{Me6})_3ClI_2$ (**4**) along with the crystallographic characterization of the byproduct $In_3(Ar^{Me6})_3I_2{\cdot}THF$ (**3**). The structures of **2** and **3** show clearly that using freshly prepared $LiAr^{Me6}$ has a large effect on the reaction outcome as the presence of "LiI" derived from the synthesis of $LiAr^{Me6}$ does not lead to the formation of the cubane $In_8(Ar^{Me6})_4$ (**1**) but instead yields products that contain the iodide ion. The structure of compound **3** is closely related to the byproduct $In_4(C(SiMe_3)_3)_4$ obtained from the stoichiometric reaction between InBr and $LiC(SiMe_3)_3$. The fact that a similar reaction using the lithium aryl reagent $LiAr^{Me6}$ yields **2** instead of $In_4(Ar^{Me6})_4$ can be rationalized by the different steric requirements of the *m*-terphenyl ligand in comparison to tris(trimethylsilyl)methyl. If the reaction between InCl and $LiAr^{Me6}$ is carried out using excess InCl, the subhalides $In_3(Ar^{Me6})_3ClI$ (**4**) and $In_4(Ar^{Me6})_4Cl_2I_2$ incorporating both chloride and iodide can be obtained depending on the relative amount of InCl used. The latter mixed-halide compound can also be synthesized by the reaction of InCl with *in situ* prepared $LiAr^{Me6}$ in toluene. Computational analysis of the parent cubane In_8H_4 demonstrates that its bonding can be conveniently described with interactions amongst four symmetry-equivalent In–In–H fragments. The frontier orbitals of In_8H_4 show both electron donor and acceptor properties, which suggests that the cluster $In_8(Ar^{Me6})_4$ might react with small molecules akin to $Sn_8(Ar^{Me6})_4$.

APPENDIX A. Supplementary data

The supplementary information includes IR, UV-Vis, ^1H and $^{13}C\{^1H\}$ NMR spectra for $LiAr^{Me6}$, **2** and **4**, additional crystallographic data for **2**, localized orbitals of **1′**, and *xyz*-coordinates of optimized structures of **2**, **4**, and **1′**. CCDC 1400650, 1400651, and 1420621 contain the supplementary crystallographic data for **2**, **3**, and **4**. These data can be obtained free of charge via http://www.ccdc.cam.ac.uk/conts/retrieving.html, or from the Cambridge Crystallographic Data Centre, 12 Union Road, Cambridge CB2 1EZ, UK; fax: (+44) 1223-336-033; or e-mail: deposit@ccdc.cam.ac.uk.

AUTHOR INFORMATION

Corresponding Authors

*P. P. Power: pppower@ucdavis.edu, H. M. Tuononen: heikki.m.tuononen@jyu.fi

ACKNOWLEDGMENTS

We thank the U. S. Department of Energy Office of Basic Energy Sciences (FG02-07ER46475) and the Academy of Finland (projects 136929, 253907, and 272900) for support of this work. P. V. thanks the Fulbright Center for a personal scholarship. Laboratory technician Elina Hautakangas is gratefully acknowledged for performing the elemental analyses.

REFERENCES

[1] G. Linti, H. Schnöckel, Coord. Chem. Rev. 206–207 (2000) 285–319, doi:10.1016/S0010-8545(00)00339-8.

[2] B.E. Eichler, N.J. Hardman, P.P. Power, Angew. Chem. Int. Ed. 39 (2000) 383–385. doi:10.1002/(SICI)1521-3773(20000117)39:2<383::AID-ANIE383>3.0.CO;2-Q.

[3] M. Driess, H. Noth (Eds.), Molecular clusters of the main group elements, Wiley-VCH, Weinheim, Germany, 2004.

[4] S. Aldridge, A.J. Downs (Eds.), The group 13 metals aluminium, gallium, indium and thallium: chemical patterns and peculiarities, John Wiley & Sons Ltd., Chichester, England, 2011.

[5] H. Schnöckel, Chem. Rev. 110 (2010) 4125–4163. doi:10.1021/cr900375g.

[6] H. Schnöckel, A. Schnepf, Adv. Organomet. Chem. 47 (2001) 235–281. doi:10.1016/S0065-3055(01)47013-4.

[7] W. Uhl, Adv. Organomet. Chem. 51 (2004) 53–108. doi:10.1016/S0065-3055(03)51002-4.

[8] P. Vasko, S. Wang, H.M. Tuononen, P.P. Power, Angew. Chem. Int. Ed. 54 (2015) 3802–3805. doi:10.1002/anie.201411595.

[9] P.P. Power, Nature. 463 (2010) 171–177. doi:10.1038/nature08634.

[10] J.M. Buriak, Chem. Rev. 102 (2002) 1271–1308. doi:10.1021/cr000064s.

[11] F.H. Allen, Acta Crystallogr. Sect. B Struct. Sci. 58 (2002) 380–388. doi:10.1107/S0108768102003890.

[12] W. Uhl, M. Layh, W. Hiller, J. Organomet. Chem. 368 (1989) 139–154. doi:10.1016/0022-328X(89)85308-2.

[13] R.D. Schluter, A.H. Cowley, D.A. Atwood, R.A. Jones, J.L. Atwood, J. Coord. Chem. 30 (1993) 25–28. doi:10.1080/00958979308022744.

[14] R.D. Schluter, A.H. Cowley, D.A. Atwood, R.A. Jones, M.R. Bond, C.J. Carrano, J. Am. Chem. Soc. 115 (1993) 2070–2071. doi:10.1021/ja00058a081.

[15] W. Uhl, R. Graupner, M. Layh, U. Schütz, J. Organomet. Chem. 493 (1995) C1–C5. doi:10.1016/0022-328X(95)05399-A.

[16] P.J. Brothers, K. Hübler, U. Hübler, B.C. Noll, M.M. Olmstead, P.P. Power, Angew. Chem. Int. Ed. 35 (1996) 2355–2357. doi:10.1002/anie.199623551.

[17] W. Uhl, S. Melle, G. Geiseler, K. Harms, Organometallics 20 (2001) 3355–3357. doi:10.1021/om0102302.

[18] W. Uhl, F. Schmock, G. Geiseler, Z. Anorg. Allg. Chem. 628 (2002) 1963–1966. doi:10.1002/1521-3749(200209)628:9/10<1963::AID-ZAAC1963>3.0.CO;2-W.

[19] R.J. Wright, A.D. Phillips, N.J. Hardman, P.P. Power, J. Am. Chem. Soc. 124 (2002) 8538–8539. doi:10.1021/ja026285s.

[20] O. Serrano, J.C. Fettinger, P.P. Power, [{GaI(Ar^{Me6})}$_2$], Polyhedron. 58 (2013) 144–150. doi:10.1016/j.poly.2012.08.039.

[21] A. Ecker, E. Weckert, H. Schnöckel, Nature. 387 (1997) 379–381. doi:10.1038/387379a0.

[22] A. Schnepf, H. Schnöckel, Angew. Chem. Int. Ed. 40 (2001) 711–715. doi:10.1002/1521-3773(20010216)40:4<711::AID-ANIE7110>3.0.CO;2-K.

[23] S.T. Haubrich, P.P. Power, J. Am. Chem. Soc. 120 (1998) 2202–2203. doi:10.1021/ja973479c.

[24] C.J.F. Du, H. Hart, K.K.D. Ng, J. Org. Chem. 51 (1986) 3162–3165. doi:10.1021/jo00366a016.

[25] G.M. Sheldrick, SADABS (Siemens Area Detector Absorption Correction), 3rd ed., Universität Göttingen, Göttingen, Germany, 2008.

[26] G.M. Sheldrick, Acta Crystallogr. Sect. C Struct. Chem. 71 (2015) 3–8. doi:10.1107/S2053229614024218.

[27] TURBOMOLE V6.6, 2014, TURBOMOLE, a development of University of Karlsruhe and Forschungszentrum Karlsruhe GmbH, TURBOMOLE GmbH, since 2007; available from http://www.turbomole.com.

[28] ADF2014, SCM, Theoretical Chemistry, Vrije Universiteit, Amsterdam, The Netherlands, http://www.scm.com.

[29] J.P. Perdew, K. Burke, M. Ernzerhof, Phys. Rev. Lett. 78 (1997) 1396–1396. doi:10.1103/PhysRevLett.78.1396.

[30] J.P. Perdew, K. Burke, M. Ernzerhof, Phys. Rev. Lett. 77 (1996) 3865–3868. doi:10.1103/PhysRevLett.77.3865.

[31] J.P. Perdew, M. Ernzerhof, K. Burke, J. Chem. Phys. 105 (1996) 9982–9985. doi:10.1063/1.472933.

[32] C. Adamo, V. Barone, J. Chem. Phys. 110 (1999) 6158–6170. doi:10.1063/1.478522.

[33] F. Weigend, R. Ahlrichs, Phys. Chem. Chem. Phys. 7 (2005) 3297–305. doi:10.1039/b508541a.

[34] S. Grimme, WIREs Comput. Mol. Sci. 1 (2011) 211–228. doi:10.1002/wcms.30.

[35] S. Grimme, S. Ehrlich, L. Goerigk, J. Comput. Chem. 32 (2011) 1456–65. doi:10.1002/jcc.21759.

[36] E. Van Lenthe, E.J. Baerends, J. Comput. Chem. 24 (2003) 1142–1156. doi:10.1002/jcc.10255.

[37] E. van Lenthe, E.J. Baerends, J.G. Snijders, J. Chem. Phys. 99 (1993) 4597–4610. doi:10.1063/1.466059.

[38] E. van Lenthe, E.J. Baerends, J.G. Snijders, J. Chem. Phys. 101 (1994) 9783–9792. doi:10.1063/1.467943.

[39] E. van Lenthe, A. Ehlers, E.-J. Baerends, J. Chem. Phys. 110 (1999) 8943–8953. doi:10.1063/1.478813.

[40] S.F. Boys, Localized orbitals and localized adjustment functions, in: P.-O. Löwdin (Ed.), Quantum theory of atoms, molecules, and the solid state, Academic Press, New York, USA 1966: pp. 253–262.

[41] L. Pu, M.M. Olmstead, P.P. Power, B. Schiemenz, Organometallics 17 (1998) 5602–5606. doi:10.1021/om980697l.

[42] W. Uhl, S. Melle, Chem. Eur. J. 7 (2001) 4216–21. doi:10.1002/1521-3765(20011001)7:19<4216::AID-CHEM4216>3.0.CO;2-I.